

Observation of the Stark-tuned Förster resonance between two Rydberg atoms

I. I. Ryabtsev,* D. B. Tretyakov, I. I. Beterov, and V. M. Entin

*Institute of Semiconductor Physics
Prospekt Lavrentyeva 13, 630090 Novosibirsk, Russia
(Dated: September 16, 2009)*

Cold atoms in highly excited Rydberg states are promising candidates to implement quantum logic gates of a quantum computer via long-range dipole-dipole interaction. Two-qubit gates require a controlled interaction of only two close Rydberg atoms. We report on the first spectroscopic observation of the resonant dipole-dipole interaction between two cold rubidium Rydberg atoms confined in a small laser excitation volume. The interaction strength was controlled by fine tuning of the Rydberg levels into the Förster energy resonance using the Stark effect. The observed resonance line shapes well agree with numerical Monte-Carlo simulations.

PACS numbers: 32.80.Ee, 03.67.Lx, 34.10.+x, 32.70.Jz, 32.80.Rm

Quantum computers are among of the most intriguing challenges for researchers in different areas of physics. As no fully working quantum computer has been reported yet, many approaches are being developed simultaneously [1,2]. One of the promising approaches is a quantum computer based on neutral alkali-metal atoms trapped in optical lattices or dipole traps [2]. Each atom represents a qubit whose quantum states are the two hyperfine sublevels of the ground state.

The most challenging task with neutral atoms is to implement two-qubit quantum logic gates that provide quantum entanglement of qubits. Such gates require a controlled interaction between qubits separated by several microns. As ground-state atoms interact very weakly at such distances, it has been proposed [3,4] to excite atoms to high Rydberg states with the principal quantum number $n \gg 1$, which provides strong dipole-dipole interaction (DDI) between qubits ($\sim n^4$) [5].

The two basic proposals consider a short-term DDI of two close Rydberg atoms [3] or laser excitation of only one Rydberg atom in a mesoscopic ensemble (dipole blockade) [4]. Experimental combination of these ideas has recently resulted in the first implementation of the Controlled-NOT quantum gate with fidelity 0.73 [6] and of the entanglement with fidelity 0.75 [7] using the dipole blockade at laser excitation of two Rydberg atoms separated by 10 or 4 μm . Both experiments actually employed the van der Waals interactions enhanced by the quasi-degeneracy of the energy levels, instead of the Stark-tuned Förster resonance originally proposed in Ref. [4].

Förster resonant energy transfer due to DDI was first observed for many atoms in Ref. [8]. For cold atoms it can be precisely tuned with an electric field via Stark effect [9] and therefore is more flexible in controlling the interaction strength, otherwise one needs to change the Rydberg states or inter-atomic distance. The Stark-tuned Förster resonance is also advantageous as it in principle allows for direct measurement of the interaction strength between

two atoms by recording its spectrum in the electric-field scale and subtracting the nonresonant background signal [10]. However, it was never observed for two Rydberg atoms, to the best of our knowledge.

In this work we aimed at the first experimental observation of the Stark-tuned Förster resonance between a definite number (2 to 5) of closely spaced Rydberg atoms. Such study is a necessary pre-requisite for the future quantum gates that employ Förster resonances controlled with a weak dc electric field. In particular, line-shape analysis is important, as the resonance can be broadened by various sources of decoherence and thus may affect the fidelity of quantum gates. Coherent or incoherent evolution of the interacting Rydberg atoms, while experiencing various decoherence processes, should be precisely investigated. Electrical control of the Förster resonance can be used to adjust the phase of the collective wave function of the two qubits in quantum phase gates or to implement the dipole blockade effect [11].

Experiments with a few Rydberg atoms require special techniques for their manipulation, detection and counting. The information should be obtained by averaging over a large number of events (detection of an atom in a certain state), instead of the averaging over many atoms. In Refs. [6,7] individual atoms were manipulated with optical dipole traps, while Rydberg states were detected via photon scattering and counting after returning the atoms back to the ground state. Such technique is rather slow as it requires multiple scattering of photons. The fastest and most sensitive way to detect Rydberg atoms is the selective field ionization (SFI) [5], when the atom ionizes with almost 100% probability as soon as electric field reaches a critical value that scales as n^{-4} .

We have developed a method to separately measure the signals from $N = 1 - 5$ of the detected Rydberg atoms [10]. It is based on the SFI detector with channel electron multiplier (CEM) and on the post-selection technique. In the present work we applied this method to cold Rb Rydberg atoms in a magneto-optical trap (MOT).

The Förster resonance under study is the resonant energy transfer $\text{Rb}(37P_{3/2}) + \text{Rb}(37P_{3/2}) \rightarrow \text{Rb}(37S_{1/2}) + \text{Rb}(38S_{1/2})$ due to DDI of two or

*Electronic address: ryabtsev@isp.nsc.ru

more Rb Rydberg atoms in a small laser excitation volume. The initial energy detuning $\Delta = [2E(37P_{3/2}) - E(37S_{1/2}) - E(38S_{1/2})]/h$ in a zero electric field is 103 MHz; Δ becomes zero at 1.79 V/cm.

The experiments were performed for cold ^{85}Rb atoms in a MOT of standard configuration. Typically 10^5 – 10^6 atoms were trapped in a 0.5–0.6 mm diameter cloud. The electric field for SFI was formed by two stainless-steel plates with holes and meshes for passing the vertical cooling laser beams and the electrons to be detected. CEM output pulses from the $37S$ and $(37P+38S)$ states were detected with two independent gates and sorted according to the number N of the detected Rydberg atoms.

The excitation of Rb atoms to the $37P$ Rydberg state was realized in four steps: (i) $5S \rightarrow 5P_{3/2}$ with 780 nm cw cooling laser; (ii) $5P_{3/2} \rightarrow 8S$ with 615 nm pulsed Rhodamine 6G dye-laser; (iii) $8S \rightarrow (6P, 7P) \rightarrow 6S$ spontaneous cascade decay during 200 ns; and (iv) $6S \rightarrow 37P$ with 743 nm pulsed Ti:Sapphire laser. The pulsed lasers had a pulse width of 50 ns at a repetition rate of 5 kHz.

Small Rydberg excitation volume was formed using crossed-beam geometry [12]. The two pulsed laser beams were focused to the 9–10 μm in diameter waists and intersected at right angles inside of the cold atom cloud. The actual excitation volume, however, depends on the mutual positions of the beam waists and on the saturation of the exciting transitions. The mutual positions were aligned by scanning the 615 nm beam and by minimizing the volume size. The laser intensities were adjusted to obtain about one Rydberg atom excited per laser pulse on the average. Numerical simulation for these intensities gave the effective volume of $\simeq 5800 \mu\text{m}^3$, corresponding to a cubic volume of 18 μm in size.

Microwave spectroscopy was applied for the diagnostics of the cold Rb Rydberg atoms in the MOT [12]. The dc electric field was calibrated with 0.2% uncertainty using the Stark spectroscopy of the microwave transition $37P_{3/2} \rightarrow 37S_{1/2}$. The MOT magnetic field was not switched off, but the microwave probing allowed us to align the excitation point to a nearly zero magnetic field.

The spectra of the Förster resonances were separately recorded for various N . The measured N -atom signals are the fraction of atoms in the final $37S$ state

$$S_N = \frac{n_N(37S)}{n_N(37P) + n_N(37S) + n_N(38S)}, \quad (1)$$

where $n_N(nL)$ is the total number of nL Rydberg atoms detected by SFI during the accumulation time for the particular case of N detected Rydberg atoms. Upon complete coherent transfer from the $37P$ state to the $37S$ and $38S$ states, S_N reaches the maximum value of 0.5, as both final states are populated with equal probability. An incoherent transfer to those states leads to $S_N \leq 0.25$.

The Förster resonances recorded for $N=1-5$ at the free interaction time $t_0=3 \mu\text{s}$ are shown in Fig. 1(a). The laser polarization was chosen along the dc electric field to provide the excitation of only $37P_{3/2}(|M_J|=1/2)$ atoms

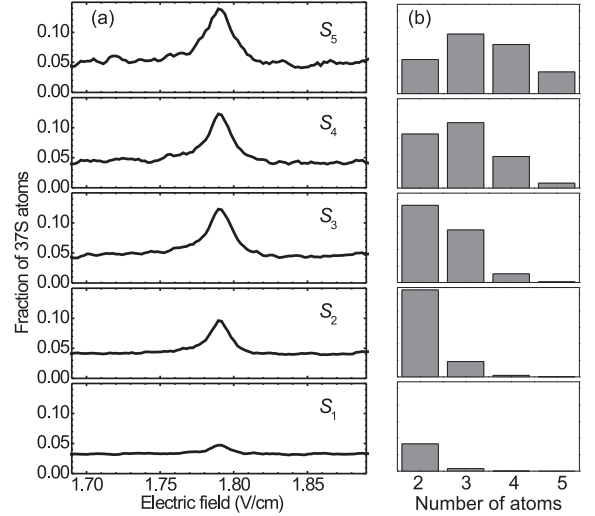


FIG. 1: (a) Experimental spectra $S_1 - S_5$ of the Förster resonance $\text{Rb}(37P_{3/2}) + \text{Rb}(37P_{3/2}) \rightarrow \text{Rb}(37S_{1/2}) + \text{Rb}(38S_{1/2})$ for 1 to 5 detected Rydberg atoms. (b) Theoretical probability distributions given by Eqs. (2) and (3) for the number of actually interacting Rydberg atoms.

from the intermediate $6S$ state. In this case a single resonance at 1.79 V/cm is observed. The height and width of the resonance grow with N , as expected. However, precise comparison between theory and experiment should be based on an adequate theoretical model for a few Rydberg atoms. In what follows, we calculate the theoretical spectra and then compare them with the experiment.

The first item to be discussed is: when we observe the spectrum S_N for N detected Rydberg atoms, does it really correspond to the spectrum ρ_N for the interaction of exactly N atoms? In our previous paper [10] we have shown that for an ideal SFI detector the signal S_N indeed gives the true spectrum ρ_N . For the nonideal detector, which detects fewer atoms than actually have interacted, various ρ_N contribute to S_N to a degree that depends on the mean number of the detected Rydberg atoms. The spectra S_N are thus a mixture of the spectra from the larger numbers of actually interacted atoms $i \geq N$ [10]:

$$S_N = \rho + e^{-\bar{n}(1-T)} \sum_{i=N}^{\infty} \rho_i \frac{[\bar{n}(1-T)]^{i-N}}{(i-N)!}. \quad (2)$$

Here ρ is a nonresonant background signal due to blackbody-radiation-induced transitions and background collisions, \bar{n} is the mean number of Rydberg atoms excited per laser pulse, and T is the detection efficiency of the SFI detector. The mean number of Rydberg atoms detected per laser pulse is $\bar{n}T$. In our experiment it was measured to be $\bar{n}T = 0.65 \pm 0.05$. According to the method developed in Ref. [10], this value along with the measured relationship between the one- and two-atom resonance amplitudes $\alpha = (S_1 - \rho) / (S_2 - \rho) = 0.27 \pm$

0.03 gives the unknown values of $\bar{n} = [\alpha/(1-\alpha) + \bar{n}T] = 1.05 \pm 0.04$ and $T = (65 \pm 5) \%$.

Equation (2) could not be directly used to describe S_N in Fig. 1(a). The reason is that at the fourth excitation step we applied a broadband pulsed laser, which excited both fine sublevels of the $37P$ state. Atoms in the $37P_{1/2}$ state do not interact but contribute to the number of the detected atoms. This leads to an additional mixing of the multiatom spectra, which can be taken into account by replacing ρ_i in Eq.(2) with a convolution of the probability to excite $i \geq 2$ atoms in a laser shot and then to find $k \geq 2$ of these in the interacting $37P_{3/2}$ state:

$$\rho_i \rightarrow \left[\sum_{k=2}^i \rho_k (p_{3/2})^k (p_{1/2})^{i-k} \frac{i!}{k!(i-k)!} \right]. \quad (3)$$

Here $p_{3/2}$ and $p_{1/2}$ are the relative probabilities to excite the $37P_{3/2}$ and $37P_{1/2}$ atoms. Calculations have shown that at our laser intensities the $6S \rightarrow 37P$ transition strongly saturates and these atoms are excited with almost equal probabilities of $p_{3/2} \approx 0.52$ and $p_{1/2} \approx 0.48$.

The resulting theoretical distributions over ρ_N , calculated with Eqs. (2) and (3) for various S_N , are presented as histograms in Fig. 1(b). These histograms show that the S_1 and S_2 spectra almost completely originate from the interaction of two Rydberg atoms. To the best of our knowledge, this is the first observation of the Stark-tuned Föster resonance for two Rydberg atoms, which is the central result of this paper. The used method thus paves a way to a detailed investigation of two-atom interactions, even when the SFI detection efficiency is far below 1. In particular, the line-shape analysis is necessary to reveal the effective coherence time at the Föster resonance to characterize the future quantum gates.

For the line-shape analysis we need to calculate various ρ_N . We applied a simplified theoretical model that considered only interactions of Rydberg atoms in the identical $37P_{3/2}(|M_J|=1/2)$ state. The operator of the DDI between two such atoms a and b is then reduced to

$$\hat{V}_{ab} = \frac{\hat{d}_a \hat{d}_b}{4\pi\epsilon_0} \left(\frac{1}{R_{ab}^3} - \frac{3}{R_{ab}^5} Z_{ab}^2 \right), \quad (4)$$

where $\hat{d}_{a,b}$ are the z -components of the dipole-moment operators of the two atoms, R_{ab} is the distance between the atoms, Z_{ab} is the z -component of the vector connecting the two atoms (z -axis is chosen along the dc electric field), and ϵ_0 is the dielectric constant. We have done the numerical Monte-Carlo simulations for $N=2-5$ interacting Rydberg atoms, randomly positioned in a small cubic volume. In this approach, the time evolution of all possible quasi-molecular states is obtained by numerical solving of the Schrödinger equation. We accounted for all possible binary resonant interactions between N atoms, as well as the always-resonant exchange interactions that may broaden the resonance. The initial positions of N

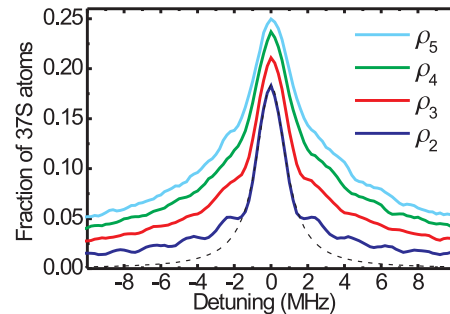


FIG. 2: (color online). Theoretical spectra ρ_N of the Föster resonance $\text{Rb}(37P_{3/2}) + \text{Rb}(37P_{3/2}) \rightarrow \text{Rb}(37S_{1/2}) + \text{Rb}(38S_{1/2})$ obtained by numerical Monte-Carlo simulations for $N=2-5$ atoms interacting for $0.515 \mu\text{s}$ and randomly positioned in a $18 \times 18 \times 18 \mu\text{m}^3$ cubic volume. The dashed line is an attempt of the Lorentz fit for ρ_2 .

atoms were averaged over 500 random realizations. Similar approach was used in Refs. [13].

Figure 2 shows the results of our calculations for 2 to 5 atoms interacted for $t_0=0.515 \mu\text{s}$ and randomly positioned in a $18 \times 18 \times 18 \mu\text{m}^3$ cubic volume. The interaction time was chosen to fit the widths of the resonances in Fig. 1(a), while the volume corresponds to the conditions of our experiment. The respective Rydberg atoms density is low and varies in the $(3-9) \cdot 10^8 \text{ cm}^{-3}$ range. The short interaction time allowed us to simplify the calculations by ignoring the effective lifetimes ($30-40 \mu\text{s}$ [14]), the motion of atoms, and the hyperfine structure (for ^{85}Rb the estimated splittings are 380, 350, and 60 kHz for $37S$, $38S$, and $37P_{3/2}$ states, respectively). Account for the hyperfine structure is impossible due to the enormously large number of quasi-molecular states, which in addition are strongly mixed by the electric field.

The theoretical spectra in Fig. 2 highlight several features. (i) At short interaction times the ultimate full width at half maximum (FWHM) is defined by the inverse interaction time $1/(t_0) \approx 1.94 \text{ MHz}$ for $N=2$. It is mainly a Fourier-transform limited width, which is larger than the estimated 0.3 MHz energy of DDI at an average distance of $10 \mu\text{m}$. The probability for two atoms to interact at much shorter distances is low, and the resonance is narrow in spite of the spatial averaging. (ii) For $N > 2$ the resonances broaden due to increase in the average energy of DDI. Averaging over the atom positions forms a resonance with broad wings and a cusp on the top, which is similar to that observed in atomic beams [10,15]. (iii) The resonance amplitude $\rho_N(\Delta = 0)$ tends to saturate at the 0.25 value. This is due to the loss of coherence and washing out of the Rabi-like population oscillations upon spatial averaging. (iv) A dashed line in Fig. 2 is an attempt to fit the ρ_2 spectrum with a Lorentz profile. It is seen that when we match the central part, the resonance wings are much broader than the Lorentz ones, due to infrequent interactions at very short distances. The commonly used Lorentz fit is thus

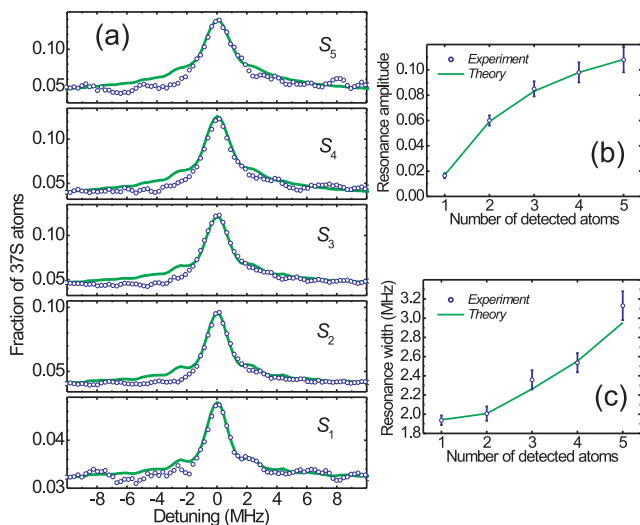


FIG. 3: (color online). (a) Comparison between theoretical (solid lines) and experimental (open circles) spectra of the Förster resonance. Theory uses the spectra of Fig. 2 and takes into account the mixing of these spectra due to finite detection efficiency and excitation of the non-interacting $37P_{1/2}$ atoms. Experiment corresponds to Fig. 1(a). (b) Theory and experiment for the resonance amplitude. (c) Theory and experiment for the resonance width.

inadequate for precise comparison between theory and experiment, especially when constant background signal is present in the experimental spectra.

Now we are able to analyze the line shapes in Fig. 1(a). In the S_1 spectrum, the FWHM in the electric-field scale is 16.4 ± 0.3 mV/cm, which corresponds to 1.94 ± 0.04 MHz. As the S_1 spectrum does not saturate, its width is defined by the effective interaction time that should be $0.515 \mu\text{s}$ according to theory. This time is shorter than $t_0 = 3 \mu\text{s}$ we set up in the experiment. The reasons for this discrepancy can be understood as follows. The free interaction time contributes about 0.3 MHz. The overall hyperfine structure contributes another 0.8 MHz. The inhomogeneous MOT magnetic field gives about 0.2 MHz. The remaining 0.7 MHz can be attributed to the parasitic ac electric fields of 5–6 mV/cm due to stray fields and ground loops. This analysis also agrees with the width of the microwave spectrum ob-

served in the 1.79 V/cm electric field.

Our Monte-Carlo simulations have shown that all above broadenings can be accounted for by simply reducing the interaction time to $0.515 \mu\text{s}$ instead of $3 \mu\text{s}$. Apparently, this is due the fact that the hyperfine, Zeeman and Stark structures of the Förster resonance lead to an effective decrease of the interaction time and are thus the main sources of decoherence.

The final theoretical spectra are shown as solid lines in Fig. 3(a). The open circles are the experimental data of Fig. 1(a) in the detuning scale. The non-resonant background level was added to theory in order to fit the experiment at the far wings of the resonance. It was used for correct determination of the resonance height. Figure 3(a) demonstrates the good coincidence of the theoretical and experimental line shapes for all N . The wings of the experimental two-atom spectra S_1 and S_2 even reproduce some of the coherent features due to population oscillations. The slight asymmetry in the red-detuned wing is attributed to the non-sharp edges of the electric-field switching in the experiment. The resonance amplitude saturates at about 0.125 value [Fig.3(b)] instead of 0.25, because half of the Rydberg atoms are excited to the non-interacting $37P_{1/2}$ state. The dependence of the amplitude on N shows perfect agreement between theory and experiment. The experimental dependence of the resonance FWHM on N is also close to theory [Fig.3(c)].

To conclude, we have observed for the first time the Förster resonance between two Rydberg atoms. Although the atom positions were not fixed, the interaction strength, the signal-to-noise ratio, and the spectral resolution were large enough for the line-shape analysis. The line shape well agrees with theory, showing that the two-atom interactions are controlled by an electric field in a predictable way. This is an important step towards implementation of the electrically-controlled neutral-atom quantum gates. The next step should be observation of coherent population oscillations at the Förster resonance, which is necessary for quantum phase gates [16].

We appreciate fruitful discussions with E. Arimondo and M. Saffman. This work was supported by the RFBR (Grant Nos. 09-02-90427 and 09-02-92428) jointly with the Consortium EINSTEIN, by the Russian Academy of Sciences, and by the Dynasty Foundation.

-
- [1] A. Galindo and M. A. Martin-Delgado, Rev. Mod. Phys. **74**, 347 (2002).
 - [2] J. J. Garcia-Ripoll, P. Zoller, and J. I. Cirac, J. Phys. B **38**, S567 (2005).
 - [3] D. Jaksch *et al.*, Phys. Rev. Lett. **85**, 2208 (2000).
 - [4] M. D. Lukin *et al.*, Phys. Rev. Lett. **87**, 037901 (2001).
 - [5] T. F. Gallagher, *Rydberg Atoms* (Cambridge University Press, Cambridge, England, 1994).
 - [6] L. Isenhower *et al.*, arXiv:0907.5552 [quant-ph].
 - [7] T. Wilk *et al.*, arXiv:0908.0454 [quant-ph].
 - [8] K. A. Safinya *et al.*, Phys. Rev. Lett. **47**, 405 (1981).
 - [9] A. Tauschinsky *et al.*, Phys. Rev. A **78**, 063409 (2008); T. J. Carroll *et al.*, Phys. Rev. A **73**, 032725 (2006); K. Afrousheh *et al.*, Phys. Rev. A **74**, 062712 (2006).
 - [10] I. I. Ryabtsev *et al.*, Phys. Rev. A **76**, 012722 (2007); Erratum: Phys. Rev. A **76**, 049902(E) (2007).
 - [11] T. Vogt *et al.*, Phys. Rev. Lett. **97**, 083003 (2006).
 - [12] D. B. Tretyakov *et al.*, JETP **108**, 374 (2009).

- [13] S. Westermann *et al.*, Eur. Phys. J. D **40**, 37 (2006);
B. Sun and F. Robicheaux, Phys. Rev. A **78**, 040701(R)
(2008); K. C. Younge *et al.*, Phys. Rev. A **79**, 043420
(2009).
- [14] I. I. Beterov *et al.*, Phys. Rev. A **79**, 052504 (2009).
- [15] J. R. Veale *et al.*, Phys. Rev. A **54**, 1430 (1996).
- [16] S. Osnaghi *et al.*, Phys. Rev. Lett. **87**, 037902 (2001).